Proc. Natl. Conf. Theor. Phys. **37** (2012), pp. 233-242

Mg-DOPED TiO_2 FOR DYE-SENSITIVE SOLAR CELL: AN ELECTRONIC STRUCTURE STUDY

TRAN VAN NAM, NGUYEN THUY TRANG AND BACH THANH CONG
Faculty of Physics, Hanoi University of Science, 334 Nguyen Trai, Thanh Xuan, Hanoi

Abstract. *Recently, there has been a renewed interest in TiO_2 anatase as charge transfer layer in dye-sensitized solar cells (DSSC). In this work, the electronic structure of Mg-doped TiO_2 anatase was explored in the framework of density functional theory (DFT). The results showed that the substitution of ions Mg^{2+} for ions Ti^{4+} was quite easy in comparison with non metalic doping case. It induced small lattice expansions about 0.3% along a and b axis and 0.1% along c axis which can be explained in terms of internal stress around the impurity site and the anisotropic softy of the material.The effects of Mg impurity on the bulk and surface electronic structures were also discussed in details. It caused a negative shift of the conduction band edge -1.16 eV and 1.142 for bulk and surface respectively. The Fermi level was also shifted 1 eV to the negative energy. Such effects were suggested to improve short-circuit current J_{SC} of DSSCs but decrease the open-circuit voltage V_{OC}.*

I. INTRODUCTION

Recently, dye-sensitized solar cells (DSSCs) has emerged as a brilliant candidate for high efficiency photoelectric devices which required simple fabrication technology and possibly low cost [1]. The most important component of a DSSC is a film of TiO2 nanocrystals mixed with dye-sensitized molecules. It plays the crucial role in harvesting solar energy and generating photoelectric current. Therefore, TiO_2 has been intensively studied on purpose of increasing energy conversion efficiency.

Doping TiO_2 is a promissing way to improve DSSC efficiency because it can easily shift the band edge and Fermi level of the material and thus change the electron transfer properties [2].For example, the band gap of TiO_2 was 0.89 eV narrowed by S doping because of impurity states at the top of valence band [3]. Iodine doping moved the mixed states of Ti 3d and O 2p 0.16 eV to higher energy and thus reduced the band gap of the material [4]. Tian et al reported their observation of positive shift of the Fermi level in N doping case which consequently increased the open circuit voltage of DSSCs. Al, W-codoping [5] was reported to improve both open-circuit voltage V_{OC} and short-circuit current J_{SC} of DSSCs by suppressing dark current and improving electron trap-detrap mechanism, respectively. More recently, Liu et al. [6] and Feng et al. [7] proposed Nb- and Ta-doped TiO_2 nanomaterials for fabricating DSSCs. The Nb-doped TiO_2 photoanode [8] exhibited a negative shift of the flat band potential of TiO_2 and improved short-circuit current. Meanwhile, Ta-doped TiO_2 nanowire based DSSCs [9] have an open-circuit voltage improved owing to the positive shift of the TiO_2 Fermi level.

Information on electronic structure provides a good guideline to optimize efficiency of DSSCs via doping way. Our work was aimed at getting a deep insight into the electronic

structure of a Mg doped TiO_2 anatase material in the framework of density functional theory (DFT). Mg is of the alkaline earth metallic series which were used to dope into TiO_2 anatase in order to improved photoactivities of the material [10]. The results in the literature showed that Mg is the best one of the series which can substitute for Ti in bulk. In this paper, effects of Mg doping on electronic structure as well as electron photo-injection and transportation will be discussed on the base of our ab initio calculation results.

II. CACULATION DETAILS

This research was in the framework DFT. The Kohn-Sham equation is solved by self-consistent field (SCF) scheme with convergence criterion of total energy 10^{-6} Ha (10^{-4} eV). Exchange correlation potential formulated by Pedrew and Wang (PWC) was employed [11]. We used a double-numeric quality basis set with polarization functions (DNP). MonkhorstPack k-point meshes [12] of 3x3x3 and 2x4x1 were used for bulk and surface calculation respectively. The self-consistent electron potential terms were all electron Coulomb potentials which included relativistic effects of core electrons. Relaxation processed were done until the residual forces were below 0.002 Ha/$\mathring{A}$ and maximum energy change below 10^{-5} Ha. Such a Kohn-Sham equation and SCF process were applied to the two following models. A *P1* symmetric supercell of 2x2x1 $I4_1/amd$ unit cells (Fig. 1a, b) with three dimension periodic boundary condition (PBC) was used for bulk calculations. In order to model doped bulk materials, one site of Ti was substituted by one impurity atom, i.e. one Mg atom. Then the stoichiometric formula of the doped material is $Ti_{15}MgO_{32}$ which is corresponding to 6.67% doping case. The second model was for (110) surface. It was composed of a TiO_2 slab which was cut along (110) direction and 8 Å thick embedded into vacuum which was 28Å thick (Fig. 2a, b, c). Stoichiometric formula of doped surface was $Ti_{15}MgO_{30}$ which means two-oxygen-vacancy surface.

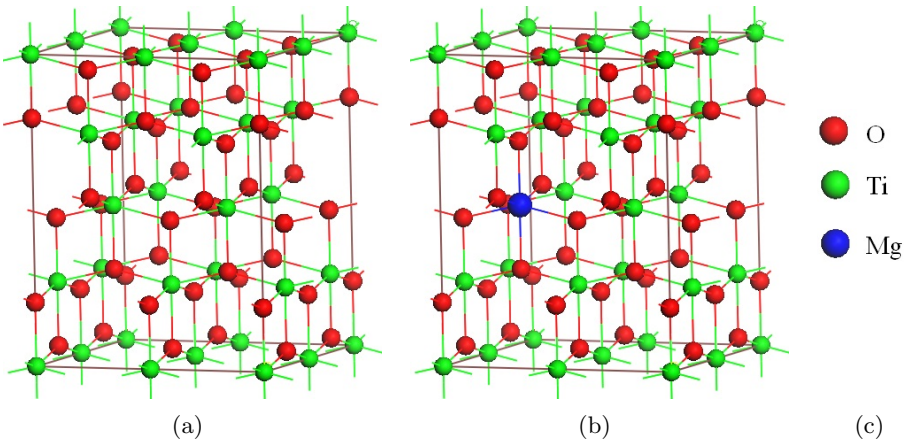

Fig. 1. Supercell structure of pure TiO_2 (a) and doping Mg (b)

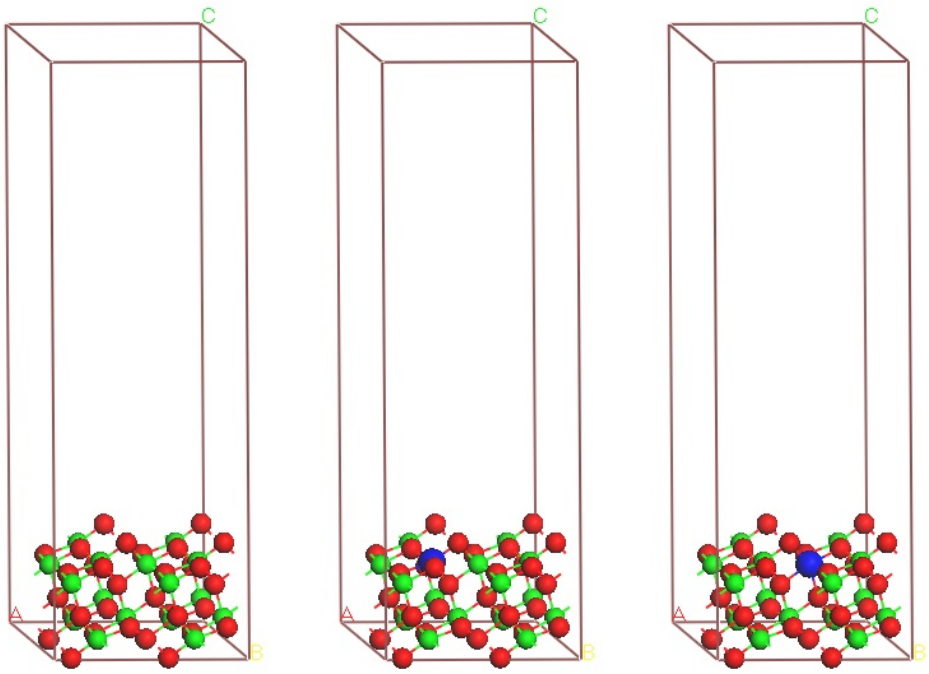

(a) (b) (c)

Fig. 2. Supercell for modeling TiO_2 surface anatase(101): non-doped surface (a), substitute Mg for Ti_{5C} (b) and substitute Mg for Ti_{6C} (c)

III. RESULT AND DISCUSSION

III.1. Calculations on pure TiO_2 material

Fig. 3a shows the band structure of pure anatase TiO_2. The calculated band gap is ${E_g}^{undoped} = 2.12$ eV, which is smaller than the experimental one ${E_g}^{exp} = 3.2$ eV [13]. The optimized cells parameters are a=b=3.813Å c=9.78 which are larger than the experiment ones a=b=3.78Å c=9.19Å [14]. Those are well-known failures of local density approximations in DFT. The top of valence band (VB) approximately locates near the G-point and the bottom of the conduction band (CB) locates at the G-point, which means that TiO_2 anatase has an indirect band gap. Our result is in good agreement with those ones of Ju-Young Park et al, which predicted an indirect band gap of 2.1 eV [15] and of Yin et al which gave rise to an indirect band gap of 1.88 eV [16]. Fig. 4a represents the density of states for pure TiO_2. The core states are highly-dense and locate in a narrow energy band between -26.5 eV and -23 eV. They are primarily oxygen 2p states (91%). There are also 9% of them titanium 2p, 3d states. The VB locates between -13.5 eV and -7 eV. It is composed mainly of the oxygen 2p states (83%) and titanium 3d states (17%). The CB ranging from -5.5 eV to -3 eV originates from titanium 3d states (92%) with the remaining small amount of oxygen 2p. According to this, the overlap

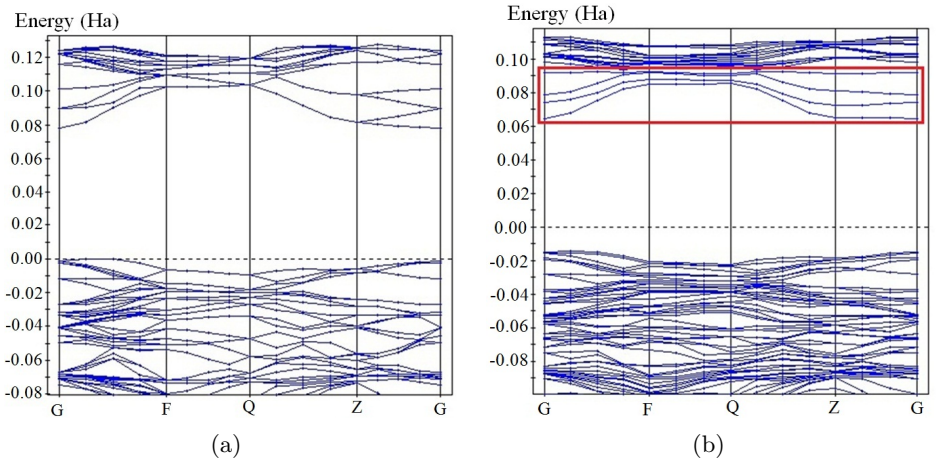

Fig. 3. Band structure of bulk TiO_2: non-doped (a) and doped Mg (b) (1 Ha=27.21138 eV)

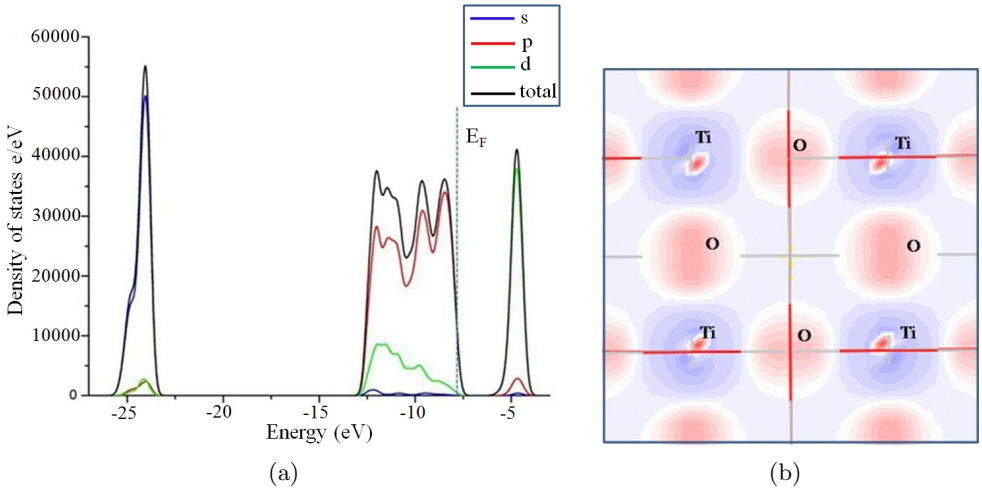

Fig. 4. Density of states of pure TiO_2 anatase (a) and Its electron deformation density (b)

between Ti states and O states is so small that the Ti-O bonding should be considered to be strongly polarized or ionic. The electron deformation density $\Delta\rho$ shown in Fig. 4b gives a good visualization of the ionic nature of TiO_2 crystal bonding. Here, $\Delta\rho$ is the difference between electron density of TiO_2 crystal $\rho_{crystal}$ and the total of electron density of isolated atoms ρ_i:$\Delta\rho = \rho_{crystal} - \sum i\rho_i$. The blue region around Ti atom is corresponding to $\Delta\rho < 0$, i. e. electron donating, and the red one around O atom is

corresponding to $\Delta\rho > 0$, i. e. electron accepting. There is no shared electron region which is corresponding to covalence bonding between O and Ti.

The limitation of crystal by (110) surface gave rise to significant change in band structure as observed from our calculation on vacuum slab supercell (Fig. 5a). It is should be noted that there are two oxygen vacancies on the as-built surface which would corresponding to 4-electrons doping if there were no change in oxidization state of Ti. Actually, these electron-impurity states do not appear in the calculated band structure. We suggest that these excess electrons are oxidized by surface Ti^{4+} ions. Consequently, the proportion of Ti 3d states between VB and CB is two times increased approximately (in case of bulk TiO_2 the contributions of Ti 3d states is 46% in VB and 54% in CB, on the contrary the proportion is 64% and 36% in case of TiO_2 surface) as shown in Ti 3d partial DOS (Fig.5b). According to this, it is believe that Ti^{4+} ions were deoxidized to Ti^{3+} as observed by previous experiments [5]. There is a nearly separated band at the bottom of the CB which was not observed in bulk TiO_2. It belongs to surface Ti 3d states as deduced from the partial DOS analysis (Fig. 5). We assign the separation of surface Ti 3d band to the transformation of octahedron-like to pyramid-like coordination at surface due to surface oxygen vacancies.

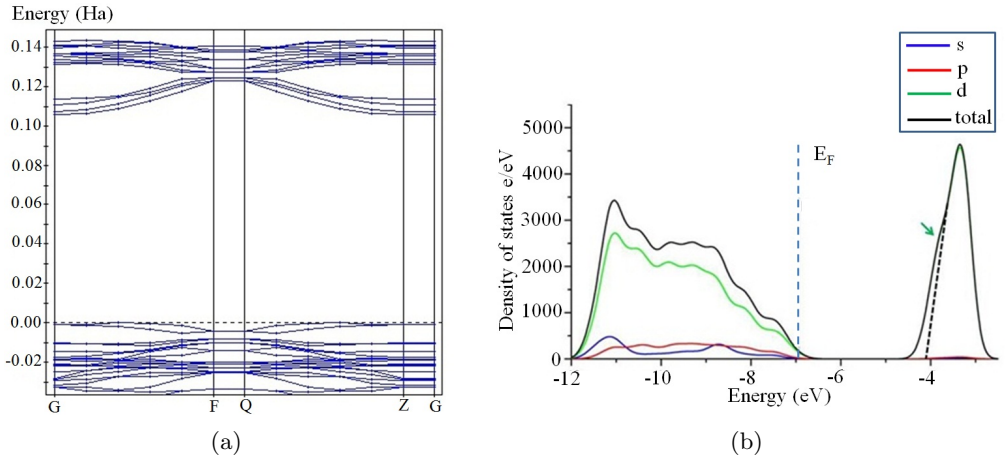

Fig. 5. Band structure (a) and partial DOS of surface Ti atoms (b).

III.2. Calculations on doped material

For the doped material, we calculated the substitution energy $E_{sub} = E_{Mg-doped} + E_{Ti} - E_{Non-dop} - E_{Mg}$. The substitution energy 8.2 eV for bulk material which is smaller than that of P substitution (12.08 eV) implies that Mg substitution reaction is easier than P one [17]. In contrast, the substitution energy is negative and quite large in value in case of surface site substitution, indicating that the substitution reaction can naturally occur. Alkaline earth doped TiO_2 compounds were prepared by Yuexiang Li et al [10]. It was observed that the substitution was the easiest for Mg^{2+} case while Be^{2+} tended to insert into interstitial site, Ca^{2+} was harder to substitute Ti^{4+} and able to induce lattice

deformation. The large ions, i. e. Ba^{2+} and Sr^{2+} hardly insert into crystal lattice and stayed on surface only.

The calculated average unit cell sizes are 0.3% increased for a and b and 0.1% for c, i.e. a=b=3.825 Å c= 9.792 Å when one Ti in 2x2x1 supercell is substituted by one Mg (Table. 1). The increase of lattice parameter can be explained in term of local lattice distortion induced by impurity site. The ionic radius of Mg^{2+} $r_{Mg^{2+}} = 0.86$ Å [18] is larger than Ti^{4+} $r_{Ti^{4+}} = 0.74.5$ Å [18]. Then the substitution of the larger ion for the smaller ion led to an internal stress around the impurity site. On the other hand, the structure of TiO_2 anatase can be described by a coordination of octahedral TiO_6 (Fig. 6a) in which there are double octahedron layers stacking alternatively along c axis (Fig. 6b). There are more empty rooms between layers than within layer. Thus, the crystal is more compressible along c axis than a and b axis. On the base of ab initio calculations, W. Y. Yin et al addressed c axis as the soft axis of TiO_2 anatase crystal because the Youngs modulus along c direction is more than two time smaller than that one along inplane directions [16]. As a result, the impurity enlarged the MnO_6 octahedron and induce an internal stress. As described above this internal stress should increase Ti-O bondlength along c axis, i. e. Ti-$O_{1,2}$ more strongly than those ones along a and b axis, i. e. Ti-$O_{3,4,5,6}$. Our result is on the same track with such a Youngs modulus analysis that Ti-$O_{3,4,5,6}$ bondlengths are decreased while the Ti-$O_{1,2}$ ones are 1.05% increased. However, this bondlength increasing is compensated by empty rooms between octahedral layers. Then c is increased less than a and b.

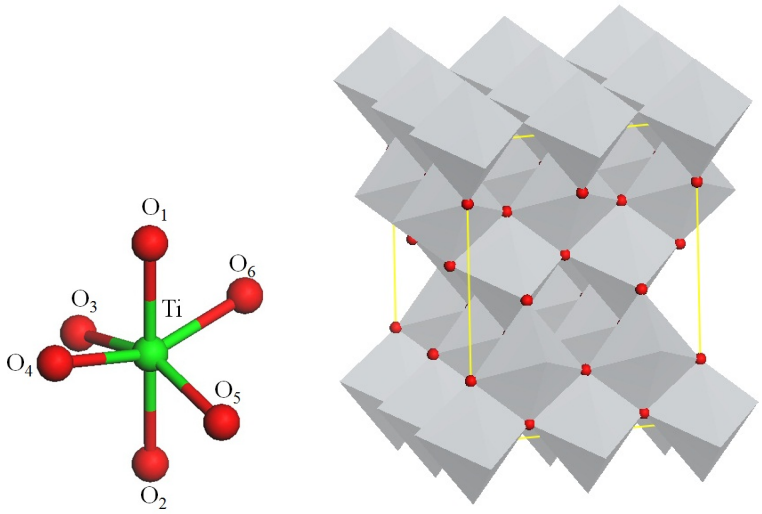

(a) Octahedral (b) Arrangement of octahedrals

Fig. 6. illustration for octahedral layer structure of bulk TiO_2

The band structure of doped TiO_2 is shown in Fig. 3b with band gap $E_g{}^{doped} = 2.15$ eV, which is increased 0.03 eV 0.14% in comparison with pure crystal. There were two possible origins of the band gap enlargement: the contribution of Mg states right above

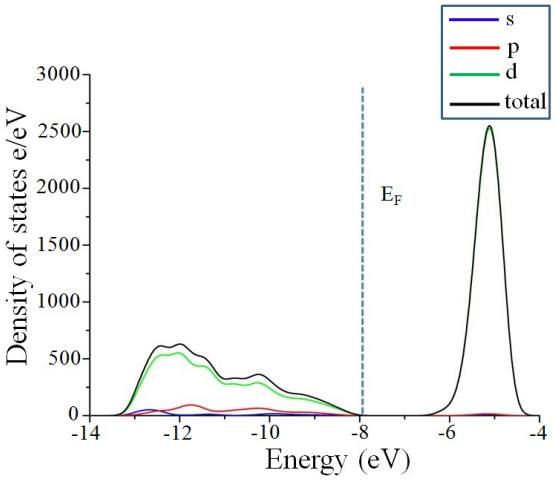

Fig. 7. Partial DOS of Mg atom.

Table 1. Lattice parameters of bulk TiO_2

axis	Non-doped TiO_2 (Å)		Mg-doped-TiO_2 (Å)		
	Ti-O	Lattice constants	Ti-O	Mg-O	Lattice constants
a	1.956	7.625	1.950	2.035	7.65
b	1.956	7.625	1.950	2.035	7.65
c	2.006	9.78	2.027	2.149	9.792

VB or below CB and the impurity-induced lattice distortion. The first origin was excluded because there is no Mg band found at the top of VB or the bottom of CB (see Mg partial DOS in Fig. 7). The second origin was taken into account. It was shown by ab initio calculations of W. Y. Yin et al and L. Thulin et al that increasing stress along inplane direction increases band gap of TiO_2 while increasing stress along c direction reduces the gap [19]. They addressed such relation to the change in Ti-O bondlength and bondangle without detail consideration on this problem. On the other hand, as discussed above, the impurity-induced stress leads to the 1.05% change in Ti-O along c axis and the enlarging of MnO_6 octahedron, the Ti-O along a and b axis is decreased 0.3% in this case. The consequent change in band gap is 0.14% increasing which agree with the behavior of the material when increasing stress along c direction.

Despite of that the substitution of Mg for surface Ti naturally occurs, there are two sites for such a surface substitution: Ti_{5C} (surrounded by 5 oxygen atoms) and Ti_{6C} (surrounded by 6 oxygen atoms) (Fig. 2b, c). Total energies (table 2) suggest that Ti_{5C} site is energetically more preferable than Ti_{6C} one. In this case, there is an acceptor band above the valance band (Fig 8a) which belongs to surface oxygen atoms around impurity site (Fig 8b).

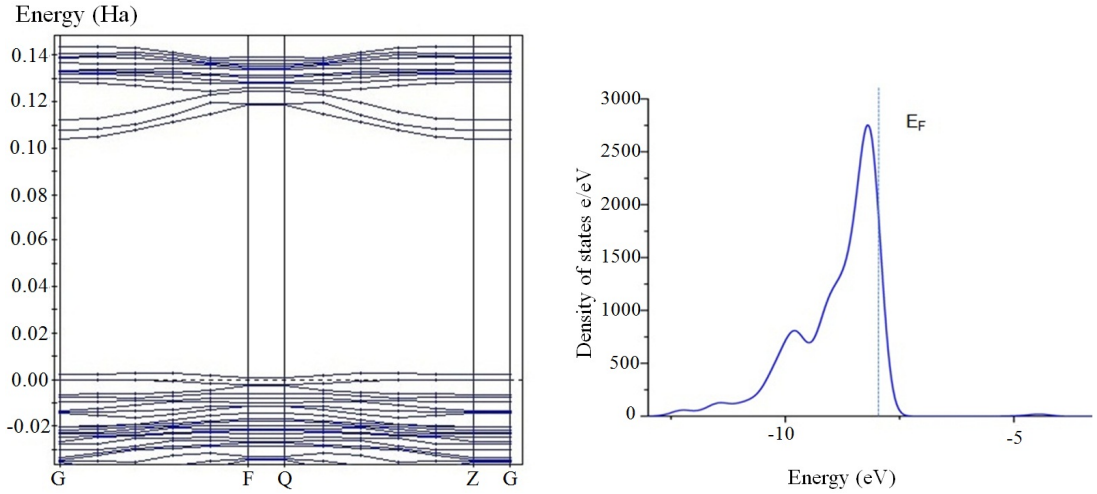

Fig. 8. Band structure (a) and partial DOS of O atoms on the Mg-doped TiO_2 surface (b)

Table 2. Total energy of Mg-doped TiO_2 surface

	Mg is substituted at Ti_{5C}	Mg is substituted at Ti_{6C}
Energy	-99484.378 eV	-99484.097 eV

III.3. Mg doping and efficiency of DSSCs.

In order to understand effect of doping on energy transformation effect of DSSC, it is necessary to mention short circuit current J_{SC} and open circuit voltage V_{OC}. JSC strongly depends on the photo-exciting possibility of electron from the highest occupied molecular orbital (HOMO) of dye molecules to the bottom of TiO_2 CB. Thus, the driving force of electron injection is the energy difference between the dye HOMO and the TiO_2 CB bottom [20]. Lowering down the CB bottom of TiO_2 is a useful way to increase J_{SC} because it make electron easier to hope from dyes HOMO to TiO_2 CB. V_{OC} is determined by the difference between Fermi level of TiO_2 and redox potential of mediator (see Fig. 9a). The higher the TiO_2 Fermi energy is the large V_{OC} is and vice versa. Adjusting Fermi level and CB band of TiO_2 is a way of optimizing DSSC efficiency. We take a note from our results that Mg doping makes the CB bottom 1.16 eV (in bulk) and 1.142 eV (on surface) negatively shift (Fig. 9b,c) which increase the driving force of electron injection from dye to TiO_2. Unfortunately, negative shifts of CB bottom were usually accompanied by negative shift of Fermi level. In our case, the Fermi level is shifted 0.812 eV (in bulk) and 1.062 eV (on surface) to the negative pole.

Another important thing is related to the trap-detrap mechanism of electron transportation. In DSSC, when an electron is injected into the CB of TiO_2, it quickly relaxes to the bottom of this band. As shown above, because the bottom of CB is made of Ti

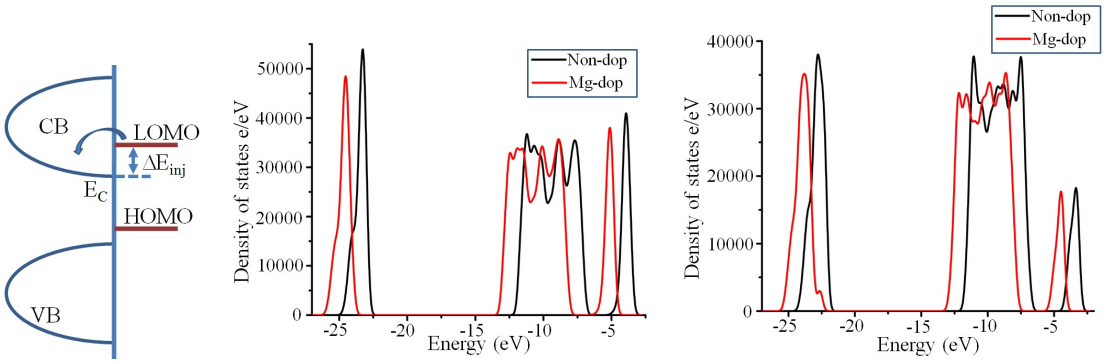

(a) Driving force (b) Bulk TiO_2 (c) TiO_2 surface

Fig. 9. The dependence of driving force on the edge of CB (a) and the negative shift of CB when doping Mg (a,b)

surface states, injected electrons are naturally trapped at Ti surface sites. The trap-detrap mechanism of injected-electron transportation in nano TiO_2 proposed by Juan Bisquert et al[21] seems to be in good agreement with our calculation by this way. However, when there is a Mg impurity atom on the surface, induced acceptor states right above the VB also can trap injected electrons as well as increase the possibility of recombination. In this way, Mg doping tends to reduce rather than increase short current.

IV. CONCLUSION

In conclusion, our work gained a deep in side into the effect of Mg doping on structure and electronic structure of TiO_2 anatase. Impurity atoms gave rise to an internal stress which, in turn, increases Ti-O bondlength along c axis but decreasing the ones along a and b axis. As a result, the band gap was enlarged. Simutaneously, the negative shift of the conduction band edge -1.16 eV and 1.142 for bulk and surface respectively were observed . The Fermi level was also shifted 1 eV to the negative energy. Such effects were suggested to improve short-circuit current J_{SC} of DSSCs but decrease the open-circuit voltage V_{OC}. Besides, Mg impurity produced recombination centre which migh reduce the short-circuit current.

ACKNOWLEDGEMENT.

We would like to thank Project no QG 12.01 financed by Vietnam National University, Hanoi and TN 12.08 financed by Hanoi University of Science for support.

REFERENCES

[1] M. Gratzel, *Philos. Trans. R. Soc. A* **365** 993 (2007) .
[2] H. Imahori, S. Hayashi, T. Umeyama, S. Eu, A. Oguro, S. Kang, Y. Matano, T.Shishido, S. Ngamsinlapasathian, S. Yoshikawa, *Langmuir* **22** 11405 (2006).
[3] Long, Run; English, Niall J.; Dai, Ying, *Journal of Physical Chemistry C*, **113** (40): 1764-1770.
[4] Run Long, Ying Dai, Baibiao Huang, *Computational Materials Science* **45** 223228 (2009).

[5] Kyung Hyun Ko, Young Cheol Lee, Young Jin Jung, *Journal of Colloid and Interface Science* **283** 482487 (2005).
[6] X. Lu, X. Mou, J. Wu, D. Zhang, L. Zhang, F. Huang, F. Fu, S. Huang, *Adv. Funct.Mater.* **20** 509 (2010).
[7] X. Feng, K. Shankar, M. Paulose, C. Grimes, Angew. *Chem. Int. Ed.* **48** 8095 (2009).
[8] Tsvetkov Nikolay, Liudmila Larina, Oleg Shevaleevskiyb and Byung Tae Ahn, *Energy Environ. Sci.* **4** 14801486 (2011).
[9] Jia Liua, Haotian Yanga,Weiwei Tana, Xiaowen Zhoua, Yuan Lina, *Electrochimica Acta* **56** 396400 (2010).
[10] Yuexiang Li, Shaoqin Peng, Fengyi Jiang, Gongxuan Lu and Shuben Li, *J. Serb. Chem. Soc.* **72** (4) 393402 (2007).
[11] Perdew J. P. and Wang Y. (1986), *Phys. Rev. B,* **33**(12), pp. 8800-8802.
[12] Monkhorst, H. J.; Pack, *J. D. Phys. Rev. B* **13** 5188 (1976).
[13] L. Wan, J.F. Li, J.Y. Feng, W. Sun, Z.Q. Mao, *Materials Science and Engineering B* **139** 216220 (2007).
[14] C. J. Howard, T. M. Sabine, and F. Dickson, Acta Crystallogr, *Sect. B: Struct. Sci.* **47** 462 (1991).
[15] Ju-Young Park, Changhoon Lee,Kwang-Wo o Jung , and Dongwoon Jung, Bull. *Korean Chem. Soc.* **Vol. 30**, No. 2 (2009).
[16] Wan-Jian Yin,Shiyou Chen, Ji-Hui Yang, Xin-Gao Gong, Yanfa Yan and Su-Huai Wei, *Appl. Phys. Lett.* **96**, 221901 (2010).
[17] Run Long, Niall J. English, *Journal of Physical Chemistry C*, **113** (21): 9423-9430.
[18] R. D. Shannon. *Acta Cryst A* **32:** 751767 (1976).
[19] Lukas Thulin and John Guerra, *Physical Review B* **77**, 195112(2008).
[20] Anders Hagfeldt, Gerrit Boschloo, Licheng Sun,*Lars Kloo and Henrik PetterssonChem. Rev.* **110**, 65956663 (2010).
[21] Juan Bisquert, *J. Phys. Chem. C*, **111** (46), pp 1716317168 (2007).

Received 30-09-2012.